

Incommensurate charge-stripe correlations in the kagome superconductor $\text{CsV}_3\text{Sb}_{5-x}\text{Sn}_x$

Linus Kautzsch,¹ Yuzki M. Oey,¹ Hong Li,² Zheng Ren,² Brenden R. Ortiz,¹ Ram Seshadri,¹ Jacob Ruff,³ Terawit Kongruengkit,¹ John W. Harter,¹ Ziqiang Wang,² Ilija Zeljkovic,² and Stephen D. Wilson¹

¹Materials Department, University of California Santa Barbara, California 93106 United States

²Department of Physics, Boston College, Chestnut Hill, MA 02467, USA

³CHESS, Cornell University, Ithaca, New York 14853, USA

(Dated: October 21, 2022)

We track the evolution of charge correlations in the kagome superconductor CsV_3Sb_5 as its parent charge density wave state is destabilized. Upon hole-doping, interlayer charge correlations rapidly become short-ranged and their periodicity is diminished along the interlayer direction. Beyond the peak of the first superconducting dome, the parent charge density wave state vanishes and incommensurate, quasi-1D charge correlations are stabilized in its place. These competing, unidirectional charge correlations demonstrate an inherent electronic rotational symmetry breaking in CsV_3Sb_5 , and reveal a complex landscape of charge correlations across the electronic phase diagram of this class of kagome superconductors. Our data suggest an inherent $2k_f$ charge instability and competing charge orders in this class of kagome superconductors.

Charge correlations and the nature of charge density wave (CDW) order within the new class of $AV_3\text{Sb}_5$ ($A=\text{K, Rb, Cs}$) kagome superconductors [1–4] are hypothesized to play a crucial role in the anomalous properties of these compounds. Hints of pair density wave superconductivity [5, 6] as well as signatures of orbital magnetism [7–10] in these compounds are all born out of a central CDW state [11–13]. The CDW order parameter itself is theorized to host both primary, real and secondary, imaginary components [14], each of which is thought to play a role in the anomalous properties observed in $AV_3\text{Sb}_5$ compounds.

The real component of the CDW state manifests primarily as a 2×2 reconstruction within the kagome plane driven via a $3\mathbf{q}$ distortion into either star-of-David (SoD) or (its inverse) tri-hexagonal (TrH) patterns of order [15]. In-plane distortions are further correlated between kagome layers [11, 16–18], either through correlated phase shifts of the same distortion type between neighboring layers, via alternation between distortion mode types, or a combination of both [19].

The parent CDW state of CsV_3Sb_5 forms a lattice whose average structure is comprised of a modulation between SoD and TrH distortion modes along the interlayer c -axis below $T_{CDW} = 94$ K [17, 20, 21]. Locally, the CDW supercell arises from a nearly degenerate mixture of states with $2 \times 2 \times 4$ and $2 \times 2 \times 2$ cells whose selection is dependent upon subtle effects such as thermal history and strain conditions imparted during growth [22, 23]. While the interlayer stacking details are a low energy feature susceptible to small perturbations, the dominant feature of the CDW in all cases is the 2×2 reconstruction in the ab -plane, representing a commensurate charge modulation on the kagome lattice.

Upon cooling deeper into the CDW state, hints appear of a staged behavior within the in-plane charge modulation, suggestive of another coexisting or competing CDW instability. Scanning tunneling microscopy (STM)

measurements resolve commensurate, quasi-1D charge stripes that form near $T \approx 60$ K and coexist with the 2×2 in-plane CDW order [12], while transient reflectivity [24] and Raman measurements [25] also resolve a shift/new modes in the lattice dynamics near this same energy scale. Sb NQR and V NMR measurements further observe a chemical shift in this temperature regime [26], demonstrating a structural response to a modified CDW order parameter—one potentially driven by competing CDW correlations.

Further supporting the notion of a nearby charge state competing with the parent CDW order is the rapid suppression of thermodynamic/transport signatures of the CDW state in CsV_3Sb_5 under moderate pressure [27, 28] or via small levels of hole-substitution [29]. By substituting $\approx 6\%$ holes per formula unit, the CDW state seemingly vanishes in thermodynamic measurements, whereas superconductivity undergoes a nonmonotonic response and generates two superconducting domes. Understanding the evolution of charge correlations between these two domes stands to provide important insights into the origin of the unconventional coupling between CDW order and superconductivity reported in CsV_3Sb_5 .

Here we track the evolution of charge correlations in $\text{CsV}_3\text{Sb}_{5-x}\text{Sn}_x$ as holes are introduced via Sn-substitution and the in-plane 2×2 CDW state is suppressed. X-ray diffraction data resolve that very light Sn-substitution ($x = 0.025$) suppresses CDW correlations, and the CDW immediately becomes short-ranged along the interlayer axis. Increased hole-doping reveals continued shortening of interlayer correlations and the suppression of in-plane 2×2 CDW order; however, this suppression of commensurate 2×2 order is accompanied by the emergence of competing quasi-1D, incommensurate charge correlations ($x = 0.15$). Parallel STM measurements also observe the persistence of low-temperature quasi-1D charge stripes in the absence of 2×2 CDW order

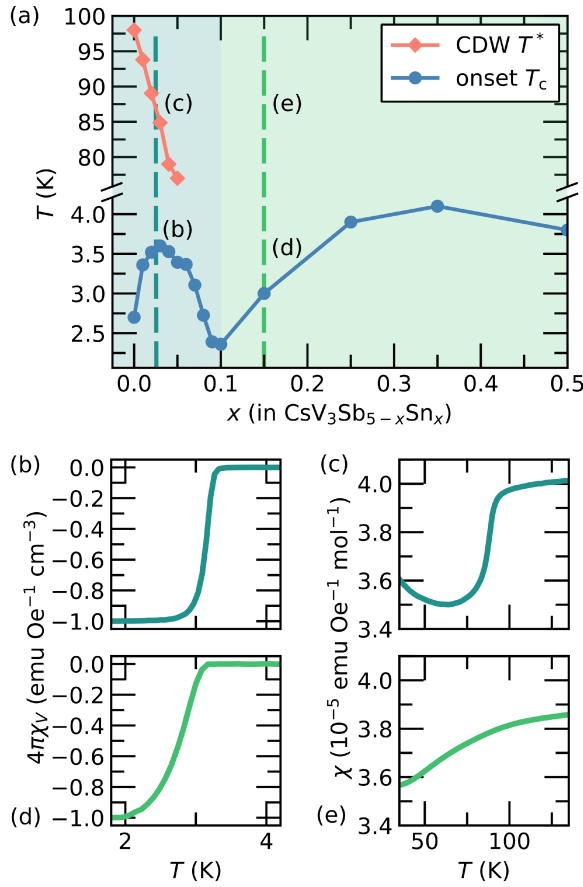


FIG. 1. (a) Electronic phase diagram of Sn-doped CsV_3Sb_5 showing the evolution of both CDW and SC order with hole-doping. Data are reproduced from Ref. [29]. Panels (b) and (c) show susceptibility data characterizing the superconducting and CDW states of the $x = 0.025$ composition in the first SC “dome” and panels (d) and (e) show susceptibility data characterizing the superconducting and CDW states of the $x = 0.15$ composition in the second SC “dome”.

[30]. Our data unveil a complex landscape of competing charge correlations that evolve across the superconducting domes of this material.

$\text{CsV}_3\text{Sb}_{5-x}\text{Sn}_x$ crystals were grown using conventional, flux-growth techniques [31] and characterized via magnetization measurements in a Quantum Design Magnetic Properties Measurement System (MPMS3). Synchrotron x-ray diffraction experiments were performed at the ID4B (QM2) beamline, CHESS [31], and STM data were acquired using a Unisoku USM1300 STM at approximately 4.5 K [31]. To understand the evolution of charge correlations across the electronic phase diagram of $\text{CsV}_3\text{Sb}_{5-x}\text{Sn}_x$, two Sn concentrations were chosen as shown in Fig. 1 (a). The first $x = 0.025$ concentration possesses both a superconducting state with an enhanced T_c and a clearly observable CDW transition as shown in Figs. 1 (b) and (c). The second $x = 0.15$ concentration retains a SC phase transition but the thermodynamic sig-

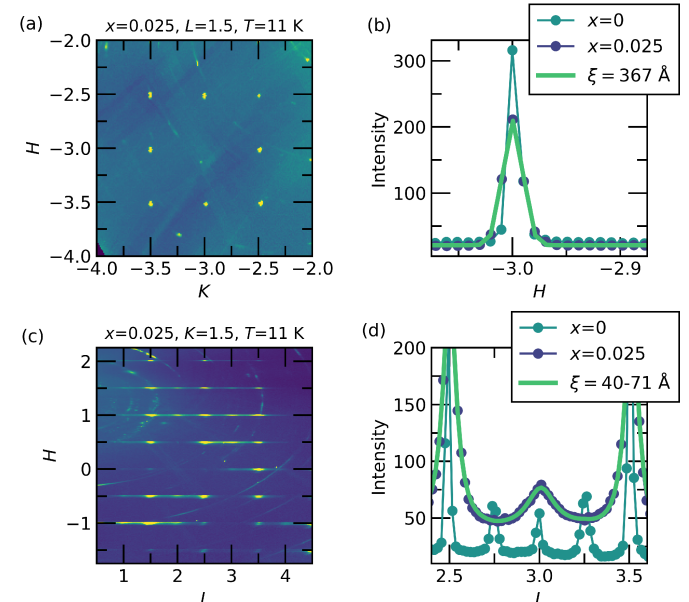


FIG. 2. (a) Map of x-ray scattering intensities in the $(H, K, 1.5)$ -plane for the $x = 0.025$ sample at $T = 11$ K. (b) One dimensional H -cuts through the $(-3, -2.5, 1.5)$ position for both $x = 0$ and $x = 0.025$. Solid lines are Gaussian fits to the data. (c) Map of x-ray scattering intensities in the $(H, 1.5, L)$ plane for the $x = 0.025$ sample. (d) One-dimensional L -cuts along $H = 1$ for both the $x = 0$ and $x = 0.025$ samples. Solid lines are pseudo-Voigt fits for the $x = 0.025$ sample with the Gaussian component fixed to the instrument’s resolution.

nature of 2×2 CDW order in susceptibility has vanished as shown in Figs. 1 (d) and (e).

Looking first at the $x = 0.025$ crystal, maps of x-ray diffraction data were collected with representative data plotted in Figs. 2 (a) and (b). Fig. 2 (a) plots scattering within the $(H, K, 1.5)$ -plane. Reflections centered at $(H, K) = (0.5, 0.5)$ -type positions indicate that the parent 2×2 in-plane CDW order remains in the $x = 0.025$ compound. However, interlayer correlations are altered. Fig. 2 (c) plots scattering within the $(H, 1.5, L)$ -plane, showing that c -axis correlations shift to substantially shorter-range and center primarily at the $L = 0.5$ positions. This marks a suppression of $2 \times 2 \times 4$ correlations in the undoped material and a transition into a short-range CDW state whose \mathbf{q} vectors match those of undoped $(\text{K}, \text{Rb})\text{V}_3\text{Sb}_5$ [11].

The in-plane correlation lengths associated with CDW peaks in the $x = 0.025$ sample are slightly reduced, shortening from resolution-limited in the undoped material to $\xi_H = 367 \pm 6$ Å. Interplane correlation lengths shorten dramatically, reducing to $\xi_L = 70 \pm 2$ Å. Weak reflections also appear at integer L positions with shorter correlation lengths $\xi_L = 40 \pm 2$ Å. Similar weak, integer L reflections also appear in the undoped $x = 0$ compound, and their presence likely reflects that interlayer correlations

are heavily impacted by local minima upon rapid cooling [22, 23, 25]. The difference in correlation lengths between half-integer and integer L CDW reflections in the $x = 0.025$ sample reflects two distinct patterns of c -axis modulation present prior to reaching a doping level where the CDW becomes truly two-dimensional.

At this small doping level, the immediate disappearance of $L=0.25$ type peaks demonstrates a reduction in the mixed character of CDW order and suggests a switch from a state with modulating SoD and TrH order into one with phase-shifted planes of a single distortion type, similar to $(\text{K},\text{Rb})\text{V}_3\text{Sb}_5$ [20]. This crossover into another CDW phase at light doping may drive the formation of the first SC dome in the phase diagram of $\text{CsV}_3\text{Sb}_{5-x}\text{Sn}_x$; however a quantitative refinement of the isolated $2 \times 2 \times 2$ CDW state will be required to further understand the mechanism.

Examining charge correlations outside of the nominal 2×2 CDW phase boundary, x-ray scattering data for the $x = 0.15$ sample are plotted in Fig. 3. Panels (a) and (b) show a representative schematic of the scattering and data in the $(H, K, -0.5)$ -plane. Data collected at half-integer L values indicate a superposition of three quasi-1D patterns of charge scattering. This can be understood in a model of charge correlations forming preferentially along one unique in-plane axis (i.e. H or K), reducing the six-fold rotational symmetry to two-fold, and forming three domains rotated by 120° in real space. These quasi-1D domains vanish upon warming as shown in Fig. 3 (d), similar to CDW domain formation in the undoped $x = 0$ system observed in optics and STM measurements [7, 12].

Looking at scattering from a single domain, charge correlations form an incommensurate state with $\mathbf{q}_{inc} = 0.37$ along a preferred in-plane axis. This is illustrated via a representative cut along H plotted in Fig. 3 (c). Within the (H, K) -plane, correlations along \mathbf{q}_{inc} are short-ranged with $\xi_H = 66 \pm 2 \text{ \AA}$ and are substantially longer-ranged orthogonal to the direction of modulation with $\xi_K = 176 \pm 7 \text{ \AA}$ (Fig. 2(e)). As shown in Fig. 3 (f), the peak of these quasi-1D correlations is centered at the $L = -0.5$ position with a short-correlation length of $\xi_L = 18 \pm 1 \text{ \AA}$, reflecting an anti-phase modulation between neighboring kagome layers correlated only between neighboring V-planes. Analysis of scattering attributed to the other two domains is presented in the supplementary information [31].

To further investigate the local evolution of charge correlations, STM measurements were performed on the $x = 0.15$ sample at $T = 4.5 \text{ K}$. Figs. 4 (a) and (b) show STM topographs of the Sb surface over different fields of view where dark hexagonal defects correspond to individual Sn dopants. Counting these defects is consistent with the expected Sn concentration $x = 0.15$. One-dimensional, stripe-like features are apparent in the STM topograph (Figs. 4 (a) and (b)), which can be more eas-

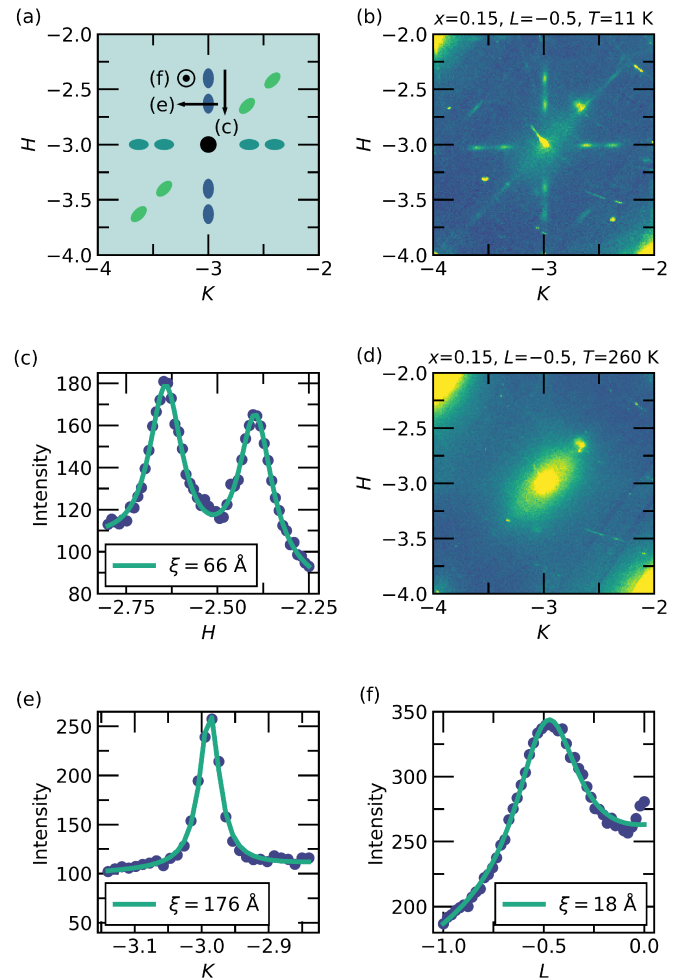


FIG. 3. (a) Schematic of x-ray scattering in the (H, K) -plane about a representative zone center for the $x = 0.15$ sample. Scattering from three domains is illustrated and cut directions for corresponding panels are labeled. (b) Map of x-ray scattering intensities for $x = 0.15$ at $T = 11 \text{ K}$ plotted about $(H, K, -0.5)$ (c) One dimensional cut along H as illustrated in panel (a), (d) Map of x-ray scattering intensities for $x = 0.15$ at $T = 300 \text{ K}$ (e-f) One dimensional cuts along K and L as illustrated in panel (a). Solid lines are the results of pseudoVoigt fits to the peak lineshapes with the Gaussian component constrained to the instrument's resolution.

ily quantified via the Fourier transform plotted in Fig. 4 (c). In this Fourier map, quasi-1D correlations are observed along one of the atomic Bragg peak directions with a map-averaged $\mathbf{q}_{inc} \approx 0.2$, reminiscent of the previously identified $4a_0$ charge stripes in the undoped system [12]. The superlattice peaks at the 2×2 (or $2a_0$) CDW positions are notably absent. This is further demonstrated via the line cuts through the Fourier map along the three lattice directions, where no scattering peaks can be observed at 2×2 positions (Fig. 4 (d)).

To gain insight into the electronic band structure,

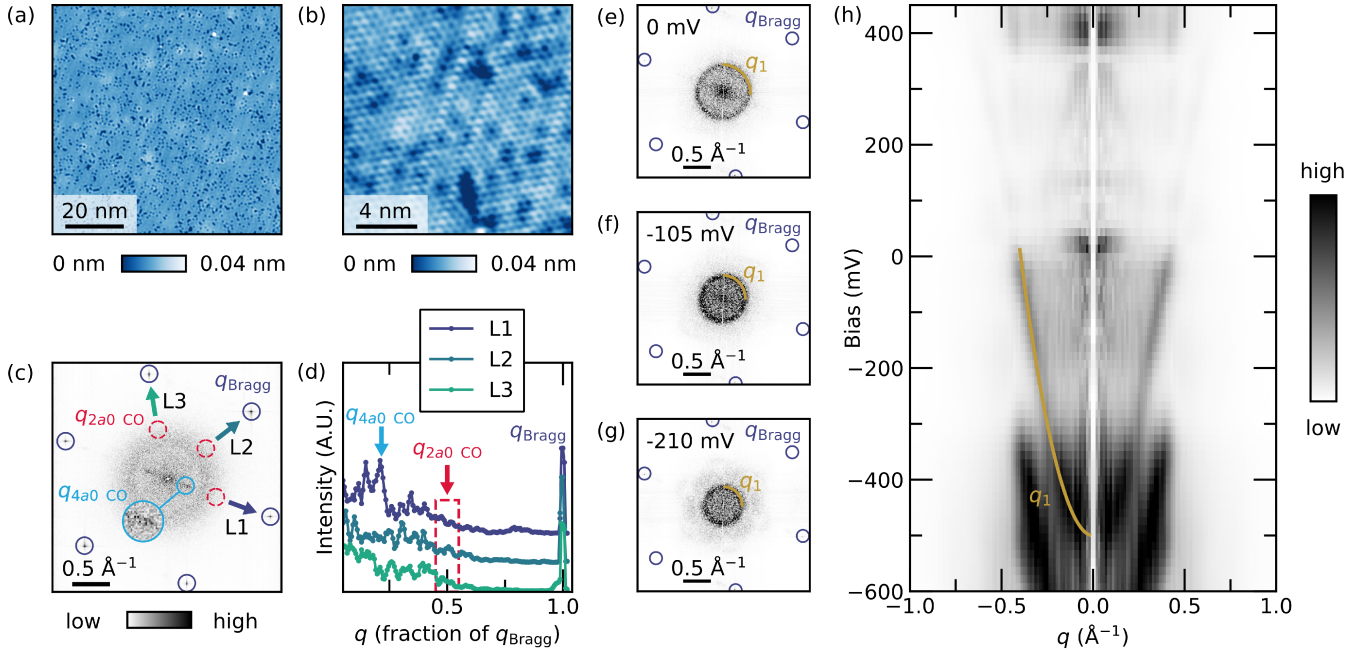


FIG. 4. (a) and (b) show STM topography images of CsV_3Sb_5 , (c) Fourier transform of the STM topography showing the presence of quasi-1D, $4a_0$ -like, order and the absence of 2×2 ($2a_0$) correlations, (d) One dimensional line cuts through the Fourier map in panel (c), (e-g) Quasiparticle interference spectra collected at 0 mV, -105 mV, and -210 mV biases respectively. The circular scattering from q_1 due to the Sb p_z states is marked. (h) The dispersion of the QPI pattern showing the bottom of the Sb p_z band has risen to ≈ -500 meV.

quasiparticle interference (QPI) imaging is plotted in Fig. 4. Fourier transforms of STM dI/dV maps in Figs. 4 (e)-(g) show the electron scattering and interference pattern as a function of increasing STM bias (binding energy). The dominant dispersive scattering wave vector is the nearly isotropic central circle (labeled q_1), which arises from scattering within the Sb p_z band that crosses through E_f . Hole-doping is predicted to be orbitally-selective and should preferentially dope this band [29, 32], pushing the bottom of the band closer to E_f . Figure 4 (h) shows the resulting dispersion of q_1 , where it can be seen that the bottom of the Sb p_z band has been pushed up from below -600 meV in the $x = 0$ parent system [12] to ≈ -500 meV in the $x = 0.15$ sample. This is consistent with DFT expectations of hole-doping achieved via the replacement of in-plane Sb atoms with Sn.

The persistence of stripe-like correlations on the surface of the $x = 0.15$ sample in the absence of the 2×2 CDW state suggests that the interactions driving this surface order are linked to the formation of the quasi-1D order resolved in the bulk via x-ray scattering measurements. In STM data, the only charge correlations that break translational symmetry are inhomogeneous, incommensurate stripes, and, diffraction measurements show that incommensurate charge modulations *should be present*. We therefore hypothesize that the quasi-1D cor-

relations sampled in diffraction and STM data arise from the same instability, with the precise wave vector of the quasi-1D stripes modified by the surface in STM studies. Quasi-1D correlations were observed in STM measurements to pin at the surface below ≈ 60 K in undoped CsV_3Sb_5 [12], and estimates of the onset temperature of quasi-1D correlations in the $x = 0.15$ sample show that they form in a similar temperature range [31]. In the $x = 0$ system, coherent, quasi-1D band features appear in the differential conductance dI/dV maps at low temperature [33], reflective of a strong coupling between these correlations and the electronic structure.

The incommensurate character of the CDW correlations in the $x = 0.15$ sample stresses the importance of electron-electron interactions in this regime of the phase diagram. A $2k_f$ nesting instability can, in principle, arise once the 2×2 reconstruction of the original Fermi surface is lifted and the Fermi level is shifted downward via hole-doping. In the absence of the reconstructed 2×2 cell, the nesting wave vector should be doping dependent, and future studies at higher Sn-concentrations can test this conjecture.

More broadly, our experiments establish AV_3Sb_5 as a promising platform for the studies of charge-stripe physics and draw comparisons with the extensively studied $4a_0$ charge ordering in cuprates [34]. For example, the sizable doping dependence of charge ordering in Bi-

based cuprates [35] appears qualitatively similar to observations in $\text{CsV}_3\text{Sb}_{5-x}\text{Sn}_x$. Given the suppression of charge ordering in cuprates in the overdoped regime, it will be of interest to explore the fate of stripe-like correlations in CsV_3Sb_5 at an even higher doping level, as samples with higher Sn composition are developed in the future.

In summary, our results demonstrate a complex landscape of charge correlations in the hole-doped kagome superconductor $\text{CsV}_3\text{Sb}_{5-x}\text{Sn}_x$. Light hole-doping eliminates $2 \times 2 \times 4$ supercell charge correlations and suppresses long-range interlayer correlations. Continued hole-doping results in the suppression of the 2×2 commensurate CDW state and the striking stabilization of quasi-1D, incommensurate charge correlations. These emergent, quasi-1D correlations demonstrate an underlying electronic rotational symmetry breaking present across the phase diagram of this system and are suggestive of a $2k_f$ nesting instability at the Fermi surface. These results provide important experimental insights into competing charge correlations in the new class of AV_3Sb_5 superconductors and crucial input for modeling the unconventional interplay between charge density wave order and the low-temperature superconducting ground state.

ACKNOWLEDGMENTS

This work was supported by the National Science Foundation (NSF) through Enabling Quantum Leap: Convergent Accelerated Discovery Foundries for Quantum Materials Science, Engineering and Information (Q-AMASE-i): Quantum Foundry at UC Santa Barbara (DMR-1906325). I.Z. gratefully acknowledges the support from the National Science Foundation grant NSF-DMR 2216080. Z.W. is supported by U.S. Department of Energy, Basic Energy Sciences Grant No. DE-FG02-99ER45747 and the Cottrell SEED Award No. 27856 from Research Corporation for Science Advancement. The research reported here made use of shared facilities of the NSF Materials Research Science and Engineering Center at UC Santa Barbara DMR-1720256, a member of the Materials Research Facilities Network (www.mrfn.org). This work is based upon research conducted at the Center for High Energy X-ray Sciences (CHEXS) which is supported by the National Science Foundation under award DMR-1829070. Any opinions, findings, and conclusions or recommendations expressed in this material are those of the authors and do not necessarily reflect the views of the National Science Foundation.

REFERENCES

- [1] B. R. Ortiz, L. C. Gomes, J. R. Morey, M. Winiarski, M. Bordonel, J. S. Mangum, I. W. Oswald, J. A. Rodriguez-Rivera, J. R. Neilson, S. D. Wilson, *et al.*, New kagome prototype materials: discovery of kv3sb5 , rbv3sb5 , and csv3sb5 , *Physical Review Materials* **3**, 094407 (2019).
- [2] B. R. Ortiz, S. M. Teicher, Y. Hu, J. L. Zuo, P. M. Sarte, E. C. Schueller, A. M. Abeykoon, M. J. Krogstad, S. Rosenkranz, R. Osborn, *et al.*, Csv3sb5 : A $z2$ topological kagome metal with a superconducting ground state, *Physical Review Letters* **125**, 247002 (2020).
- [3] B. R. Ortiz, P. M. Sarte, E. M. Kenney, M. J. Graf, S. M. Teicher, R. Seshadri, and S. D. Wilson, Superconductivity in the $z2$ kagome metal kv3sb5 , *Physical Review Materials* **5**, 034801 (2021).
- [4] Q. Yin, Z. Tu, C. Gong, Y. Fu, S. Yan, and H. Lei, Superconductivity and normal-state properties of kagome metal rbv3sb5 single crystals, *Chinese Physics Letters* **38**, 037403 (2021).
- [5] H. Chen, H. Yang, B. Hu, Z. Zhao, J. Yuan, Y. Xing, G. Qian, Z. Huang, G. Li, Y. Ye, *et al.*, Roton pair density wave in a strong-coupling kagome superconductor, *Nature* **599**, 222 (2021).
- [6] J. Ge, P. Wang, Y. Xing, Q. Yin, H. Lei, Z. Wang, and J. Wang, Discovery of charge-4e and charge-6e superconductivity in kagome superconductor csv3sb5 , *arXiv preprint arXiv:2201.10352* (2022).
- [7] Y. Xu, Z. Ni, Y. Liu, B. R. Ortiz, S. D. Wilson, B. Yan, L. Balents, and L. Wu, Universal three-state nematicity and magneto-optical kerr effect in the charge density waves in av3sb5 ($a = \text{cs}, \text{rb}, \text{k}$), *arXiv preprint arXiv:2204.10116* (2022).
- [8] C. Mielke, D. Das, J.-X. Yin, H. Liu, R. Gupta, Y.-X. Jiang, M. Medarde, X. Wu, H. Lei, J. Chang, *et al.*, Time-reversal symmetry-breaking charge order in a kagome superconductor, *Nature* **602**, 245 (2022).
- [9] L. Yu, C. Wang, Y. Zhang, M. Sander, S. Ni, Z. Lu, S. Ma, Z. Wang, Z. Zhao, H. Chen, *et al.*, Evidence of a hidden flux phase in the topological kagome metal csv3sb5 , *arXiv preprint arXiv:2107.10714* (2021).
- [10] C. Guo, C. Putzke, S. Konyzheva, X. Huang, M. Gutierrez-Amigo, I. Errea, D. Chen, M. G. Vergniory, C. Felsner, M. H. Fischer, *et al.*, Field-tuned chiral transport in charge-ordered csv3sb5 , *arXiv preprint arXiv:2203.09593* (2022).
- [11] Y.-X. Jiang, J.-X. Yin, M. M. Denner, N. Shumiya, B. R. Ortiz, G. Xu, Z. Guguchia, J. He, M. S. Hossain, X. Liu, *et al.*, Unconventional chiral charge order in kagome superconductor kv3sb5 , *Nature Materials* **20**, 1353 (2021).
- [12] H. Zhao, H. Li, B. R. Ortiz, S. M. Teicher, T. Park, M. Ye, Z. Wang, L. Balents, S. D. Wilson, and I. Zeljkovic, Cascade of correlated electron states in the kagome superconductor csv3sb5 , *Nature* **599**, 216 (2021).
- [13] N. Shumiya, M. S. Hossain, J.-X. Yin, Y.-X. Jiang, B. R. Ortiz, H. Liu, Y. Shi, Q. Yin, H. Lei, S. S. Zhang, *et al.*, Intrinsic nature of chiral charge order in the kagome superconductor rbv3sb5 , *Physical Review B* **104**, 035131 (2021).

[14] T. Park, M. Ye, and L. Balents, Electronic instabilities of kagome metals: saddle points and landau theory, *Physical Review B* **104**, 035142 (2021).

[15] H. Tan, Y. Liu, Z. Wang, and B. Yan, Charge density waves and electronic properties of superconducting kagome metals, *Physical review letters* **127**, 046401 (2021).

[16] Z. Liang, X. Hou, F. Zhang, W. Ma, P. Wu, Z. Zhang, F. Yu, J.-J. Ying, K. Jiang, L. Shan, *et al.*, Three-dimensional charge density wave and surface-dependent vortex-core states in a kagome superconductor csv3sb5 , *Physical Review X* **11**, 031026 (2021).

[17] B. R. Ortiz, S. M. Teicher, L. Kautzsch, P. M. Sarte, N. Ratcliff, J. Harter, J. P. Ruff, R. Seshadri, and S. D. Wilson, Fermi surface mapping and the nature of charge-density-wave order in the kagome superconductor csv3sb5 , *Physical Review X* **11**, 041030 (2021).

[18] H. Li, T. Zhang, T. Yilmaz, Y. Pai, C. Marvinney, A. Said, Q. Yin, C. Gong, Z. Tu, E. Vescovo, *et al.*, Observation of unconventional charge density wave without acoustic phonon anomaly in kagome superconductors av3sb5 ($a = rb, cs$), *Physical Review X* **11**, 031050 (2021).

[19] M. H. Christensen, T. Birol, B. M. Andersen, and R. M. Fernandes, Theory of the charge density wave in av3sb5 kagome metals, *Physical Review B* **104**, 214513 (2021).

[20] M. Kang, S. Fang, J. Yoo, B. R. Ortiz, Y. Oey, S. H. Ryu, J. Kim, C. Jozwiak, A. Bostwick, E. Rotenberg, *et al.*, Microscopic structure of three-dimensional charge order in kagome superconductor av3sb5 and its tunability, *arXiv preprint arXiv:2202.01902* (2022).

[21] Y. Hu, X. Wu, B. R. Ortiz, X. Han, N. C. Plumb, S. D. Wilson, A. P. Schnyder, and M. Shi, Coexistence of tri-hexagonal and star-of-david pattern in the charge density wave of the kagome superconductor av3sb5 , *arXiv preprint arXiv:2201.06477* (2022).

[22] Q. Stahl, D. Chen, T. Ritschel, C. Shekhar, E. Sadrollahi, M. Rahn, O. Ivashko, M. v. Zimmermann, C. Felser, and J. Geck, Temperature-driven reorganization of electronic order in csv3sb5 , *Physical Review B* **105**, 195136 (2022).

[23] Q. Xiao, Y. Lin, Q. Li, W. Xia, X. Zheng, S. Zhang, Y. Guo, J. Feng, and Y. Peng, Coexistence of multiple stacking charge density waves in kagome superconductor csv3sb5 , *arXiv preprint arXiv:2201.05211* (2022).

[24] N. Ratcliff, L. Hallett, B. R. Ortiz, S. D. Wilson, and J. W. Harter, Coherent phonon spectroscopy and interlayer modulation of charge density wave order in the kagome metal csv3sb5 , *Physical Review Materials* **5**, L111801 (2021).

[25] S. Wu, B. R. Ortiz, H. Tan, S. D. Wilson, B. Yan, T. Birol, and G. Blumberg, Charge density wave order in the kagome metal av3sb5 ($a = cs, rb, k$), *Physical Review B* **105**, 155106 (2022).

[26] J. Luo, Z. Zhao, Y. Zhou, J. Yang, A. Fang, H. Yang, H. Gao, R. Zhou, and G.-q. Zheng, Possible star-of-david pattern charge density wave with additional modulation in the kagome superconductor csv3sb5 , *npj Quantum Materials* **7**, 1 (2022).

[27] K. Chen, N. Wang, Q. Yin, Y. Gu, K. Jiang, Z. Tu, C. Gong, Y. Uwatoko, J. Sun, H. Lei, *et al.*, Double superconducting dome and triple enhancement of t_c in the kagome superconductor csv3sb5 under high pressure, *Physical Review Letters* **126**, 247001 (2021).

[28] F. Yu, D. Ma, W. Zhuo, S. Liu, X. Wen, B. Lei, J. Ying, and X. Chen, Unusual competition of superconductivity and charge-density-wave state in a compressed topological kagome metal, *Nature communications* **12**, 1 (2021).

[29] Y. M. Oey, B. R. Ortiz, F. Kaboudvand, J. Frassinetti, E. Garcia, R. Cong, S. Sanna, V. F. Mitrović, R. Seshadri, and S. D. Wilson, Fermi level tuning and double-dome superconductivity in the kagome metal csv3sb5-xsnx , *Physical Review Materials* **6**, L041801 (2022).

[30] H. Li, H. Zhao, B. R. Ortiz, T. Park, M. Ye, L. Balents, Z. Wang, S. D. Wilson, and I. Zeljkovic, Rotation symmetry breaking in the normal state of a kagome superconductor kv3sb5 , *Nature Physics* **18**, 265 (2022).

[31] See Supplemental Information for further details.

[32] H. LaBollita and A. S. Botana, Tuning the van hove singularities in av3sb5 ($a = k, rb, cs$) via pressure and doping, *Physical Review B* **104**, 205129 (2021).

[33] H. Li, H. Zhao, B. Ortiz, Y. Oey, Z. Wang, S. D. Wilson, and I. Zeljkovic, Emergence of unidirectional coherent quasiparticles from high-temperature rotational symmetry broken phase of av3sb5 kagome superconductors, *arXiv preprint arXiv:2203.15057* (2022).

[34] R. Comin and A. Damascelli, Resonant x-ray scattering studies of charge order in cuprates, *Annual Review of Condensed Matter Physics* **7**, 369 (2016), <https://doi.org/10.1146/annurev-conmatphys-031115-011401>.

[35] E. H. da Silva Neto, P. Aynajian, A. Frano, R. Comin, E. Schierle, E. Weschke, A. Gyenis, J. Wen, J. Schneeloch, Z. Xu, *et al.*, Ubiquitous interplay between charge ordering and high-temperature superconductivity in cuprates, *Science* **343**, 393 (2014).